Preprints of the 19th World Congress
The International Federation of Automatic Control
Cape Town, South Africa. August 24-29, 2014

An Optoelectronic Artificial Skin for Contact Force Vector Estimation

Alberto Cavallo * **Andrea Cirillo** * **Pasquale Cirillo** *
Giuseppe De Maria * **Ciro Natale** * **Salvatore Pirozzi** *

* *Dipartimento di Ingegneria Industriale e dell'Informazione, Seconda Università di Napoli, Via Roma 29. 81031 Aversa, Italy (e-mail: {alberto.cavallo, andrea.cirillo, pasquale.cirillo, giuseppe.demaria, ciro.natale, salvatore.pirozzi}@unina2.it).*

Abstract:
This work proposes a novel artificial skin, developed by using the optoelectronic technology, able to estimate both normal and shear contact force components. Each sensing module is obtained with four taxels, each one constituted by an infrared Light Emitting Diode and a Photo-Detector, covered by a silicone layer that transduces the external force in a mechanical deformation, measured by the four receivers. The applied force is estimated as a suitable combination of the four voltage signals. The distributed sensor is realized by interconnecting several sensing modules with a suitably designed scanning strategy. A complete prototype, with a 6×6 matrix of sensing modules has been realized, calibrated and tested.

Keywords: Mechanical Sensors; Contact Forces Estimation; Physical Human-Robot Interaction.

1. INTRODUCTION

Today, physical interaction between robots and humans represents a particularly challenge for robotic researchers. Sensors, which are able to detect external contacts that occur between the robots and the humans and/or the environment, are used to provide cognitive characteristics to humanoid robots and to develop new communication techniques used in different fields (Argall and Billard, 2010). In particular, safety issue become of primary concern when robots and humans works in the same unstructured environment. So, unintended collisions should be avoided by anticipating dangerous situations, while the effects of actual collisions should be mitigated by having the robot react promptly so as to recover a safe operative condition.

Two different techniques are mainly used to detect external collisions. The first approach proposes a collision detection mechanism based on the estimation of the collision torques, based on the use of the dynamic model of the robot to implement a torque observer (De Luca et al., 2006; Haddadin et al., 2008). The second approach proposes a solution that allows to obtain a complete representation of the interaction forces over the entire structure of the robot, by using three sets of sensors (i.e., force/torque, inertial and tactile sensors) distributed along the kinematic chain (Fumagalli et al., 2012). This kind of approach is based on the use of suitable distributed sensors, i.e., artificial skins, to provide to a robot the sense of touch.

In the last decade, several examples of sensors that can detect contact pressure have been presented (Cannata et al., 2008; Hoshi and Shinoda, 2006; Ohmura et al., 2006a; Duchaine et al., 2009; Ulmen and Cutkosky, 2010), but only few solutions are able to estimate the three components of the force vector applied on the contact surface of the sensor by an external colliding object. Zhang et al. presented a flexible tactile sensor array for an anthropomorphic artificial hand with the capability of measuring both normal and shear force distributions, by using quantum tunneling composite as a base material (Zhang et al., 2013). Tao Liu et al. designed a 3-D tactile sensor by integrating four sensing cells, each composed of a pressure-sensitive electric conductive rubber (PSECR) and a fan-shaped pectinate circuit (Liu et al., 2009). Both the solutions use the measurements coming from four sensing cells to estimate both normal and tangential force components.

In this paper, the authors present a novel modular artificial skin sensor able to estimate both normal and shear contact force components. Each sensing module is constituted by 4 taxels [1] covered by a silicone layer that transduces the external force in a mechanical deformation, measured by the four taxels. Each taxel consists of an infrared Light Emitting Diode (LED) and a Photo-Detector (PD). The distributed sensor is realized by interconnecting several sensing modules with a suitable scanning strategy, used to obtain an high modularity and scalability for the proposed solution. The artificial skin prototype has been calibrated, and its main features have been highlighted with several tests. A video, available on author laboratory website [2], makes most considerable the obtained results.

2. SENSOR DESCRIPTION

The skin module presented in this work was developed from the same basic idea behind the tactile sensor concept

[1] The word *taxel* derives from the union of the words "tactile element".
[2] http://research.diii.unina2.it/acl/video/Skin.wmv

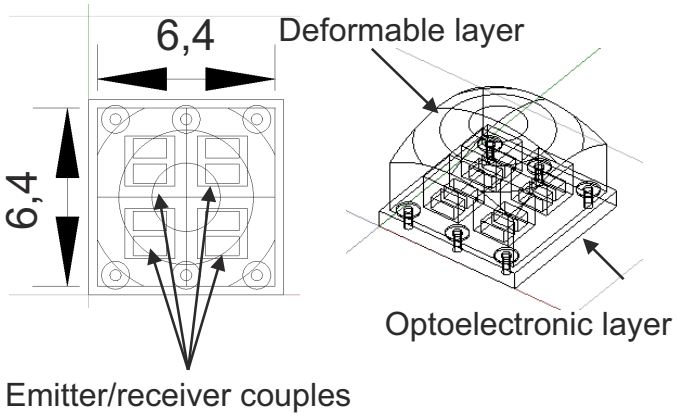

Fig. 1. CAD model of a sensing module prototype: top view on left (dimensions are in mm) and perspective view on right.

introduced in (De Maria et al., 2012), i.e., the use of optoelectronic devices to detect the local deformations, generated by a contact with an external object, of the elastic layer that covers the optoelectronic layer. With respect to the tactile sensor presented in (De Maria et al., 2012), in which 16 taxels have been used to compute through a neural network the estimation of both the three components of force vector and the three components of the torque vector, the solution proposed in this paper uses 4 optoelectronic couples to realize a single module able to estimate the three components of the force vector. The whole skin is constituted by a matrix of these sensing modules, suitably interconnected. This choice allows to estimate on the whole artificial skin all the components of the force vectors, differently from (Cirillo et al., 2012, 2013), where only the normal component of the force were estimated.

2.1 Working Principle

The skin is constituted by an interconnection of sensing modules all equal, and each capable of measuring the three components of the contact force that acts on them. Each sensing module is constituted by four taxels organized in a 2×2 matrix. A single taxel consists of an optical emitter/receiver couple spectrally matched. A deformable elastic layer is positioned above the 4 optoelectronic couples (see Fig. 1). The deformable layer has a hemispherical shape on the top side, where the interaction with external objects occurs. On the bottom side it presents 4 vacuums, of parallelepiped shape, into the material, vertically aligned with the four optoelectronic couples. For each parallelepiped cell, the facet (called reflective surface) positioned in front of the optical devices couple must have optical properties able to guarantee an high reflectivity, while the lateral walls (called absorbing surfaces), which divide neighboring taxels, have to avoid optical cross-talk effects between taxels and also to ensure the immunity against external optical disturbances. These properties can be guaranteed by using materials that allow to implement a molding of different layers, with different properties (e.g., color, thickness, surface finishing) and in different times. With this configuration, for each taxel, the emitter illuminates the reflective surface of the corresponding parallelepiped cell and the reflected light is measured by the photodetector. An external force, applied on the deformable layer, produces displacement variations for all the 4 taxels constituting a sensing element. These displacement variations produce variations of the reflected light and, accordingly, of the photocurrents measured by the photodetectors. Finally, the photocurrents are converted in voltage signals by using simple resistors. After a calibration procedure, detailed in Section 3.1, the external force components, acting on a sensing element, can be estimated with a suitable combination of the 4 measured signals. It is evident that the sensitivity and the full-scale of a sensing module depend on the hardness of the material used for the realization of the deformable layer. The complete skin is obtained suitably interconnecting several sensing modules.

2.2 Sensing Module Prototype

In order to realize the electronic layer, the optoelectronic components have been selected on the basis of previous experiences, discussions and observations detailed in (De Maria et al., 2012). In particular, the realized prototype uses optoelectronic components manufactured by OSRAM. The LED (code SFH4080) is an infrared emitter with a typical peak wavelength of 880 nm, while the detector is a silicon NPN phototransistor (code SFH3010) with a maximum peak sensitivity at 860 nm wavelength. Both the components have a viewing angle of $\pm 80°$. The conditioning electronics is only constituted by simple resistors without amplification and/or filtering stages, since the measured voltages are sufficiently high to be directly converted by using an Analog-to-Digital Converter (ADC). The material selection for the deformable layer has been made on the basis of previous experiences detailed in (D'Amore et al., 2011). In particular, a two layer plastic mold has been prepared in order to realize the deformable layer, by using black silicone for the absorbing walls and white silicone for the reflective surface. The black silicone guarantees the maximum absorption for every wavelengths and, as a consequence, to avoid cross-talk problems between taxels and ambient light disturbances. The white silicone ensures the maximum reflection for every wavelengths, increasing the sensor sensitivity. Differently from a tactile sensor, an artificial skin requires a higher full-scale and a lower sensitivity. To obtain these characteristics, a silicone with a higher hardness, with respect to the tactile sensor reported in (De Maria et al., 2012), has been selected. The selected one is the MM928, provided by ACC Silicones Europe, with a Shore hardness of 28 A and a time-cured of 24 h. The aspect ratio of the black walls between taxels has been selected in order to reduce the horizontal deformations with respect to the vertical ones. In particular, for the realized prototype, the thickness of the black walls is 0.8 mm, while the extension of the white reflecting surfaces is 1.8×1.8 mm, which results in a total size for the deformable layer of 6×6 mm. The height of the reflective surfaces from the electronic layer is 1.6 mm. The top of the deformable layer is a section of a sphere with a radius of 7 mm. The deformable layer is bonded on the electronic layer (of size 6.4×6.4 mm) by using a cyanoacrylate glue. Figure 2 reports some pictures of the sensing module components and an assembled module.

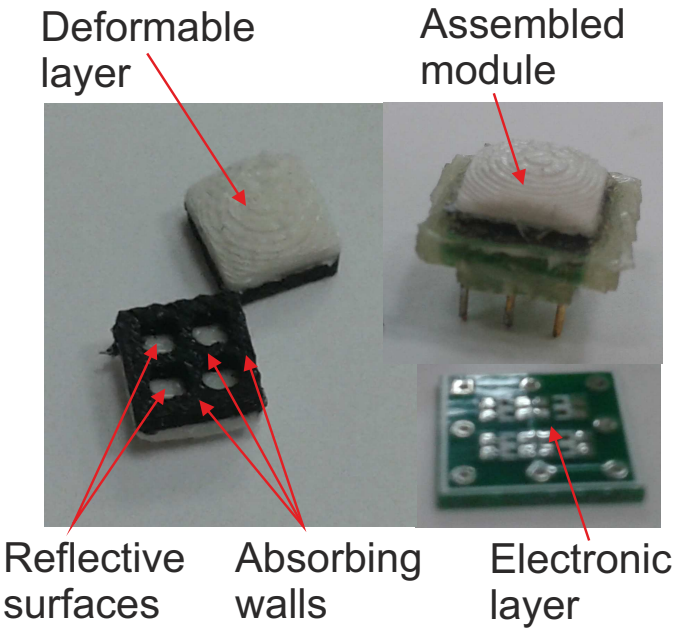

Fig. 2. Pictures of sensing module components.

2.3 Skin Prototype

A distributed skin prototype is realized interconnecting several sensing modules. The version presented in this paper is constituted by 36 modules, organized as a 6×6 matrix, for a total of 144 taxels. The sensor matrix has been developed as a shield that can be installed directly on a STM32F3 discovery board. The STM32F303 Micro-Controller Unit (MCU) provides sixteen ADC with a resolution of 12 bit: each voltage signal is digitized with two bytes and the selected MCU, with a system clock frequency of 72 MHz, represents the right trade-off between costs and performance. To ensure the scalability and the modularity of the system, a "scanning control" strategy, based on the same idea reported in (Ohmura et al., 2006b), has been adopted to realize the module interrogation by using the MCU. The basic idea is to connect the sensing modules in groups which share 4 ADC channels, and to use the digital I/O of the MCU to switch on and off, with a cyclic pattern, the sensing modules, by ensuring that in each time instant, for each group, only one taxel is turned on, while all others, which share the same ADC, are turned off (see Fig. 3). This control logic properly works since the switched off photodetectors constitute an open circuit that does not influence the measurement for the switched on photodetector. Differently from (Ohmura et al., 2006b), the sensing modules can be directly driven by the MCU digital I/O, without using an external power supply, since each LED works with a forward current of about 1 mA, widely available from a digital I/O, and the voltage supply for all components is the 3.3 V, available from the MCU. This scanning strategy allows to obtain several advantages: a reduction of the the whole sensor power consumption, since the number of modules simultaneously turned on is limited; a reduction of ADC channels required to acquire the data; a simplification of the wiring. For the realized prototype, the 36 sensing modules are divided in 3 groups. Hence, the first group is constituted of 12 sensing modules, which share 4 ADC channels and are driven by using

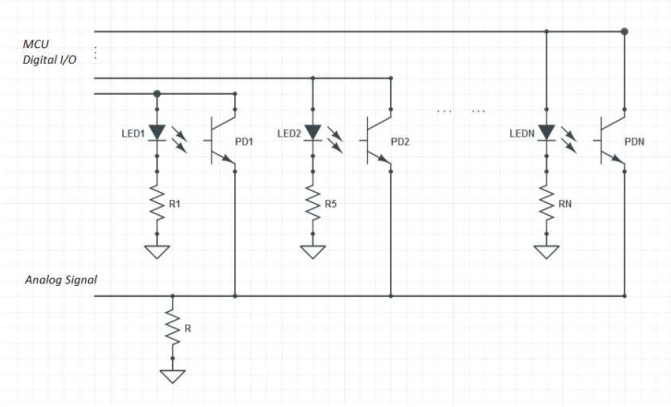

Fig. 3. Electronic scheme of the interconnections between the sensing modules and microcontrollers.

12 digital I/O. The second and the third groups share additional 4 ADC channels, respectively, for a total of 12 ADC channels. Since the second and third groups use different ADC channels, they can be driven by using the same digital I/O used for the first group. Summarizing, the 144 total taxels, which constitute 36 sensing modules organized in 3 groups, are interrogated by using 12 ADC channels (4 ADC channels shared for each group) and 12 digital I/O used to implement the scanning strategy, for a total of 25 wires (the 25−th signal is the ground) directly coming from a MCU (see Fig. 4).

Finally, the 144 voltage signals are converted and transmitted via USB connection to an hostPC with a maximum frequency of about 380 Hz. A Matlab script is running on the PC that acquires the data and computes the force components. The selected interconnection has the additional great advantage that the skin can work also if not all the sensing modules are connected or some connected modules are broken, since they appears only as open circuits, by improving the modularity of the proposed solution. The same Matlab script can be used to detect the number of the installed and/or working modules through an initialization phase. So, a virtual sensor structure can be reconstructed according to the detected modules, and used to show the information related to the estimated contact forces. Figure 4 reports a picture of the skin prototype, together with the corresponding virtual sensor structure. Note that, in the picture, 6 modules on the third group are intentionally not mounted to show how the virtual structure automatically adapts.

3. ARTIFICIAL SKIN CALIBRATION AND TESTING

The calibration of the skin prototype is based on the hypothesis that the calibration of a single module can be used also for the other ones, since all modules are realized with the same components and they are mechanically separated. Accordingly, this section presents the calibration procedure of a single module. Then the obtained calibration parameters are applied to all skin modules. The complete calibrated skin has been tested and the results are reported.

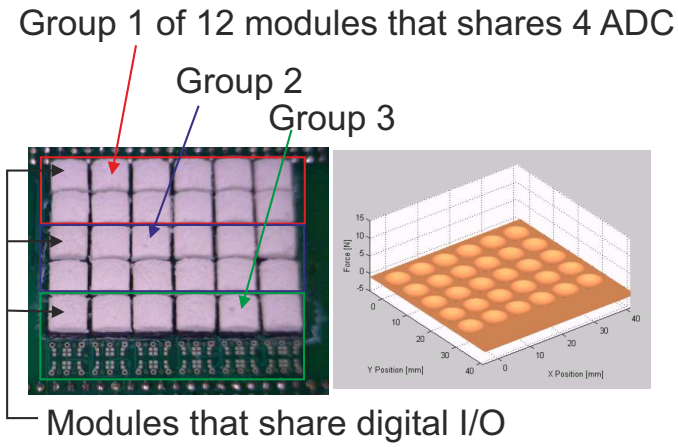

Fig. 4. Skin prototype (left) and corresponding virtual sensor structure (rigth).

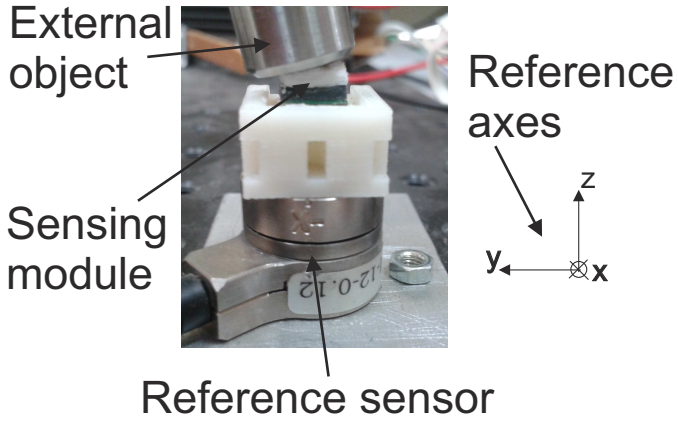

Fig. 5. Setup for the calibration of a sensing module.

3.1 Sensor Calibration

The force components can be estimated as a suitable combination of the four voltages of a sensing module. A specific calibration setup has been prepared in order to acquire at the same time the module voltages and the actual force vector, measured by using a reference sensor. Figure 5 reports a picture of the setup with the corresponding reference axes. The sensing module is mounted on a six-axes load cell used as reference sensor. The model used is the FTD-Nano-17, manufactured by ATI, with a measurement range equal to ± 12 N and ± 17 N for horizontal and vertical force components, respectively, while the measurement range for all torque components is equal to ± 120 Nmm. An operator carried out various experiments, using a stiff plane, applying different external forces and simultaneously acquiring all the voltage variations measured by the phototransistors and all the force components measured by the reference load cell. These data are acquired at a sample rate of 100 Hz. Considering the working principle described in Section 2.1, if the contact force is zero, each photodetector measures an initial voltage proportional to the light reflected by the white silicone when the deformable layer is in rest position. When an external force is applied to the deformable layer, each photodetector can present a positive or negative voltage variation with respect to the initial voltage, depending on the external force components. Figure 6 shows the voltage variations,

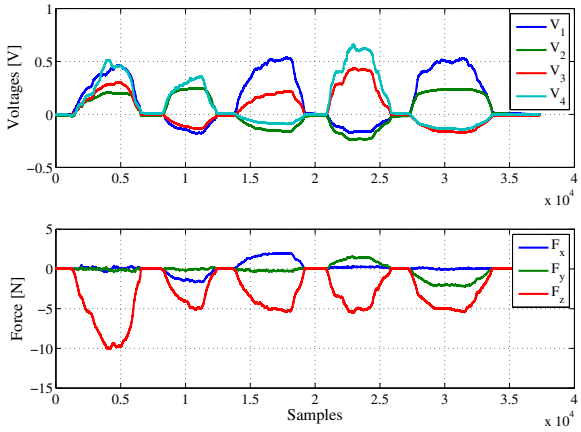

Fig. 6. Voltage variations (top) measured by the sensing module and corresponding force components (bottom) measured by the reference sensor.

measured by the sensing module, and the corresponding force components, measured by the reference sensor. It is evident that the sign of the voltage variations is related to the tangential force direction, while their amplitude to the force vector intensity. From the figure, it is also clear that the voltage variations are sufficiently high to be directly digitized without the introduction of additional amplification and/or filtering stages, as described in Section 2.2. So, if f_x, f_y, and f_z are the force components, and $\mathbf{V} = [V_1, V_2, V_3, V_4]^T$ is the vector that contains the voltage variations, the phenomenological model proposed to calibrate the sensing module is the following

$$f_x = \mathbf{k}_x^T \mathbf{V} \tag{1}$$
$$f_y = \mathbf{k}_y^T \mathbf{V} \tag{2}$$
$$f_z = \mathbf{k}_z^T \mathbf{g}(\mathbf{V}) \tag{3}$$

where the function $\mathbf{g}(\cdot)$ is simply the absolute value applied to each component of the $\mathbf{V}$ vector, and the three calibration vectors $\mathbf{k}_x$, $\mathbf{k}_y$ and $\mathbf{k}_z$ can be easily estimated with a simple least square algorithm by inverting Eqs. (1), (2) and (3), respectively, using the data set reported in Fig. 6.

The accuracy of the calibration has been validated with a second data set. In particular, the estimated force components have been computed as

$$\widehat{f}_x = \mathbf{k}_x^T \mathbf{V} \tag{4}$$
$$\widehat{f}_y = \mathbf{k}_y^T \mathbf{V} \tag{5}$$
$$\widehat{f}_z = \mathbf{k}_z^T \mathbf{g}(\mathbf{V}) \tag{6}$$

and in Fig. 7 the estimated values $\widehat{f}_x$, $\widehat{f}_y$ and $\widehat{f}_z$ are compared to the actual force components f_x, f_y and f_z measured with the reference sensor, to evaluate the calibration performance. The results show a full-scale for the normal force of about 8 N and for the tangential components of about ± 2 N, with an estimation accuracy of about 0.5 N. The full-scale can be adapted to the requirement of a specific application, by changing the mechanical properties of the deformable layer (e.g., hardness, curvature radius of the hemispherical shape). The accuracy also depends on

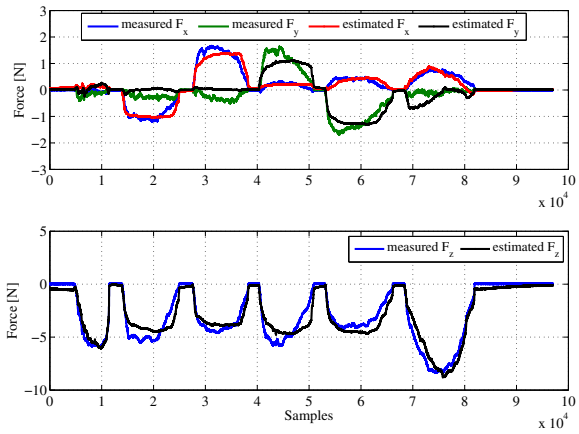

Fig. 7. Example of force vector estimation: tangential force components (top) and normal force component (bottom).

the full-scale and moreover can be improved by introducing a more complex model.

3.2 Sensor Testing

The assembled skin has been used to perform several testing. First of all, since each taxel measures a local deformation, the 144 voltages, measured with the scanning strategy described in Section 2.3, can be used as a pressure map. This map allows to discriminate multiple contacts and to reconstruct the shape of the objects in contact with the artificial skin. Figure 8 shows these features with two different experiments. In the first one, an operator acts on the sensor in two different areas (see Fig. 8(a)) and the corresponding voltage variations (reported in Fig. 8(b)) allow to reconstruct a pressure map, clearly compatible with the type of interaction. In the second experiment, the artificial skin in contact with a marker pen (see Fig. 8(c)) returns the correlated pressure map shown in Fig. 8(d). The sampling frequency (380 Hz) to interrogate the whole map allows to use these data in several control applications.

The calibration functions (4), (5) and (6), have been used in the Matlab script to estimate the force vector for each module. Hence, the same functions have been applied to the 4 voltage variations for all sensing modules, obtaining as many estimated force vectors as the sensing modules are. Figure 9 shows the estimated force vector on the virtual sensor structure, in the case of a single contact with a single sensing element. It is possible to note as the estimated force vector direction (see Fig. 9(b)) is well aligned with the contact object (see Fig. 9(a)). When a contact that covers more than one sensing module occurs, the artificial skin computes the force vector for each module involved in the contact. Figure 10(a) reports the example of an operator who interacts with the sensor in two different areas. In this case, the virtual sensor shows the force vectors estimated by all sensing modules involved in the interaction (see Fig. 10(b)). Figure 11 reports the same analysis when a marker pen interacts with the artificial skin. All the results presented in this

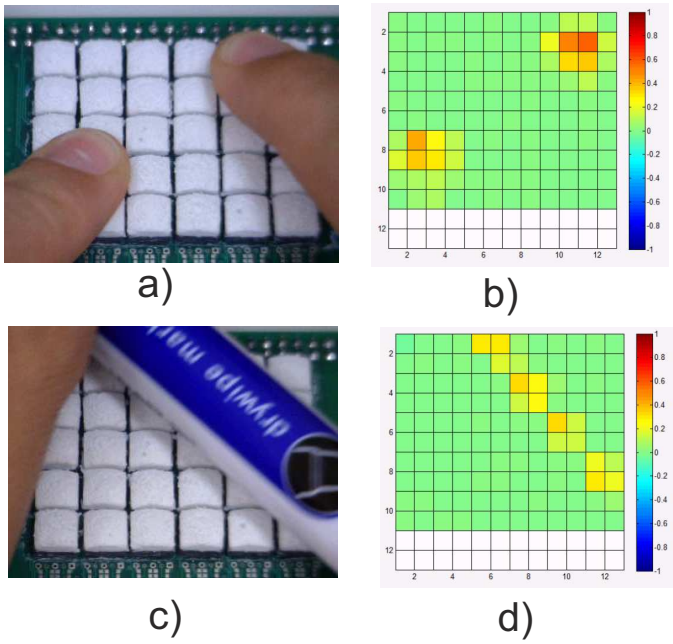

Fig. 8. Skin prototype as pressure sensor: multiple contacts (a) and its corresponding pressure map (b); marker pen shape recognition (c) and its corresponding pressure map (d).

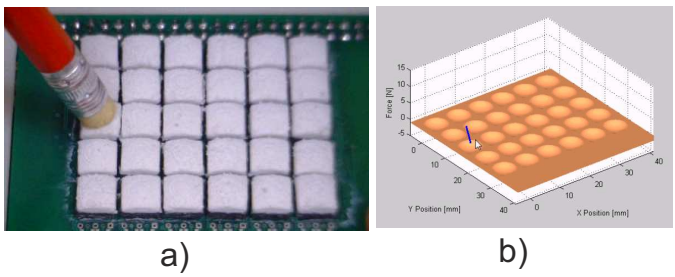

Fig. 9. Estimation of the force vector, reported on the virtual sensor structure (b), for a single contact with a single sensing module (a).

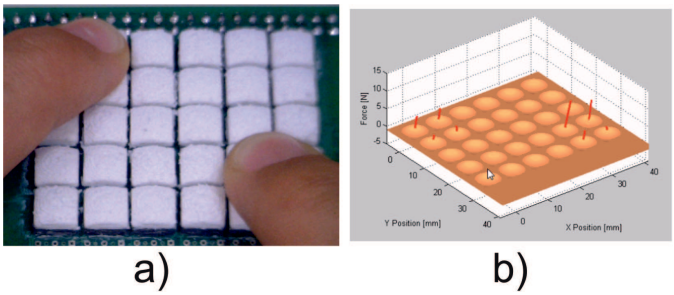

Fig. 10. Estimation of the force vectors in a multiple contacts case (a): on the virtual sensor structure (b) are reported the force vectors estimated by the single modules.

section are most considerable from the video available on the author laboratory website [3].

[3] http://research.diii.unina2.it/acl/video/Skin.wmv

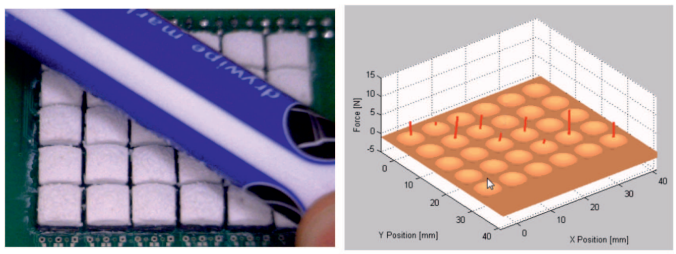

Fig. 11. Estimation of the force vectors (b) for a marker pen (a).

4. CONCLUSIONS AND FUTURE WORKS

In this paper, a novel artificial skin, based on optoelectronic technology, able to estimate all the components of the contact forces has been presented. The sensor has been realized by interconnecting sensing modules, each able to estimate the force vector. Several tests have been performed to highlight sensor features: availability of a pressure map; estimation of a force vector for each sensing module. The presented skin is still under development and the future activities will include, from a technological point of view, the realization of a conformable version by using flexible electronic boards and, from a functional point of view, the implementation of strategies able to discriminate multiple contact areas in order to estimate the force resultant for each contact area. Eventually, experiments of physical human-robot interaction will be performed installing some skin patches on a robotic arm.

ACKNOWLEDGEMENTS

This work was supported by the European Commission's Seventh Framework Programme (FP7/2007-2013) under grant agreement no. 287513 (SAPHARI project)

REFERENCES

Argall, B.D. and Billard, A.G. (2010). A survey of tactile human-robot interactions. *Robotics and Autonomous Systems*, 58, 1159–1176.

Cannata, G., Maggiali, M., Metta, G., and Sandini, G. (2008). An embedded artificial skin for humanoid robots. In *Proc. of IEEE International Conference on Multisensor Fusion and Integration for Intelligent Systems*.

Cirillo, A., Cirillo, P., De Maria, G., Natale, C., and Pirozzi, S. (2013). A proximity/contact-force sensor for human safety in industrial robot environment. In *Proc. of IEEE/ASME International Conference on Advanced Intelligent Mechatronics*, 1272–1277. Wollongong, Australia.

Cirillo, A., Cirillo, P., and Pirozzi, S. (2012). A modular and low-cost artificial skin for robotic applications. In *Proc. of 4th IEEE RAS/EMBS International Conference on Biomedical Robotics and Biomechatronics*, 961–966. Rome, Italy.

D'Amore, A., De Maria, G., Grassia, L., Natale, C., and Pirozzi, S. (2011). Silicone-rubber-based tactile sensors for the measurement of normal and tangential components of the contact force. *Journal of Applied Polymer Science*, 122, 3758–3770.

De Luca, A., Albu-Schaffer, A., Haddadin, S., and Hirzinger, G. (2006). Collision detection and safe reaction with the dlr-iii lightweight manipulator arm. In *Proc. of IEEE/RSJ Int. Conf. on Intelligent Robots and Systems 2006 (IROS2006)*, 1623–1630. Beijing, China.

De Maria, G., Natale, C., and Pirozzi, S. (2012). Force/tactile sensor for robotic applications. *Sensors and Actuators A: Physical*, 175, 60–72.

Duchaine, V., Lauzier, N., Baril, M., Lacasse, M.A., and Gosselin, C. (2009). A flexible robot skin for safe physical human robot interaction. In *Proc. of IEEE International Conference on Robotics and Automation*.

Fumagalli, M., Ivaldi, S., Randazzo, M., Natale, L., Metta, G., Sandini, G., and Nori, F. (2012). Force feedback exploiting tactile and proximal force/torque sensing. *Auton Robot*, 33, 381–398.

Haddadin, S., Albu-Schaffer, A., Luca, A.D., and Hirzinger, G. (2008). Collision detection and reaction: A contribution to safe physical human-robot interaction. In *Proc. of IEEE/RSJ International Conference on Intelligent Robots and Systems*.

Hoshi, T. and Shinoda, H. (2006). Robot skin based on touch-area-sensitive tactile element. In *Proc. of IEEE International Conference on Robotics and Automation*.

Liu, T., Inoue, Y., and Shibata, K. (2009). A small and low-cost 3-d tactile sensor for a wearable force plate. *IEEE Sensors Journal*, 9(9).

Ohmura, Y., Kuniyoshi, Y., and Nagakubo, A. (2006a). Conformable and scalable tactile sensor skin for curved surfaces. In *Proc. of IEEE International Conference on Robotics and Automation*.

Ohmura, Y., Kuniyoshi, Y., and Nagakubo, A. (2006b). Conformable and scalable tactile sensor skin for curved surfaces. In *Proc. of IEEE International Conference on Robotics and Automation*.

Ulmen, J. and Cutkosky, M. (2010). A robust, low-cost and low-noise artificial skin for human-frindly robots. In *Proc. of IEEE International Conference on Robotics and Automation*.

Zhang, T., Liu, H., Jiang, L., Fan, S., and Yang, J. (2013). Development of a flexible 3-d tactile sensor system for anthropomorphic artificial hand. *IEEE Sensors Journal*, 13(2).